Int. J. Electrochem. Sci., 11**(2016)** 7553 – 7561, doi: 10.20964/2016.09.61

International Journal of ELECTROCHEMICAL SCIENCE
www.electrochemsci.org

Short Communication

NiO Nano-Flower Sensitized by Perovskite as Photocathode for p-DSSC with Superior Hole Transfer Kinetics

Jie Qu[1,*],*YurongRen*[1], *Jia Cheng*[2], *JianningDing*[1,*],*NingyiYuan*[1]

[1]School of Materials Science and Engineering, Jiangsu Collaborative Innovation Center of Photovoltaic Science and Engineering and Jiangsu Province Cultivation base for State Key Laboratory of Photovoltaic Science and Technology, Changzhou University, Changzhou 213164, P. R. China
[2] Hunan Hua Teng Pharmaceutical Co., Ltd, Changsha 410205, P. R. China
[*]E-mail: qujie1981@cczu.edu.cn; dingjn@cczu.edu.cn

Received: 24 June2016/ *Accepted:* 19 July 2016 / *Published:* 7 August 2016

NiO nano-flower, NiO slice-cluster and NiO nanoparticles have been synthesized by a facile method. The structure and morphology of the prepared samples were characterized by X-ray diffraction (XRD) and transmission electron microscopy (TEM). The as prepared samples are used as photocathode of p-DSSC. Current-voltage (I-V) curve shows that NiO nano-flower owns the highest J_{sc} of 10 mA cm^{-2} and its efficiency can reach up to 0.84%. The UV-vis diffused reflectance spectra indicate that NiO nano-flower shows strong light scatting and diffuse reflection to enhace light harvesting. Electrochemical impendence spectroscopy (EIS), intensity-modulated photocurrent spectroscopy (IMPS), and intensity-modulated voltage spectroscopy (IMVS) further demonstrate that NiO nano-flower provides fast hole transfer, long electron life time and improved charge collection efficiency with suppressed recombination.

Keywords: p-type dye sensitized solar cell; photocathode; NiO nano-flower;perovskite; hole transfer

1. INTRODUCTION

Recently, p-type dye sensitized solar cells (p-DSSC) with sensitized p-type semiconductor as photocathode has become an attractive and growing area [1-7]. Such new type solar cell can combine with an efficient n-DSSC to construct high-efficiency tandem cells, which has a theoretical efficiency of 43% [7-8], higher than single n-DSSC or p-DSSC. However, the development of tandem DSSC is limited by the low efficiency of p-DSSC, which is caused by the intrinsically low voltage and low current [5]. Till now, the highest reported conversion efficiency of p-DSSC is 1.3 % with NiO as a photocathode[9], PMI-6T-TPA as a sensitizer, and Tris(acetylacetonato)iron(III)/(II) redox couple as a

redoxmediator, which is far away from the n-DSSCs' conversion efficiency of 12.3% [10]. How to improve the photoelectrical performance of p-DSSC has become a changelling research.

In p-DSSC, the photo excited hole was injected into the valence band of a p-type semiconductor. An excellent semiconductor should satisfy several requirements, such as a large surface area for enough dye loading, higher light scattering ability to improve the light harvesting efficiency, the film should be mechanically stable and strongly bound to the back transparent conducting electrode and so on [11-12]. p-type NiO with wide band gap of 3.5 eV was used as the most prominent photocathode material [13-18]. However, the morphology of most reported NiO was nanoparticle, which can not satisfy the requirements mentioned above. In this article, a simple method is used to synthesize different morphologies of NiO used as the scatting layer in photocathode. Compact NiO nanoparticles are used as blocking layer coated on the surface of FTO glass and organometal halide perovskites$CH_3NH_3PbI_3$ are uesd to sensitize the NiO photocathodes. Compared with NiO nanoparticles and NiO slice-cluster, NiO nano-flower shows strong light scatting to enhance light harvesting, excellent photoelectric performance and superior hole transfer kinetics.

2. EXPERIMENTS

2.1. Synthesis of the nanomaterials

NiO nano-flower:$NiCl_2$•$6H_2O$ (107.3 mg) and hexamethylenetetramine (61.3 mg) were dissoloved in sodium citrate solution (0.7 Mm, 70 ml). After stirring for 30 min, the above solution was transferred into round-bottom flask and treated at 90 ˚C for about 6h. The product was recovered and rinsed with distilled water, then ethanol. After being dried at 60 ˚C for about 24h, the as-prepared sample was calcined in an oven at 500 ˚C for 2h.

NiO slice-cluster:$NiCl_2$•$6H_2O$ (107.3 mg) and hexamethylenetetramine (61.3 mg) were dissoloved in sodium citrate solution (0.7 Mm, 70 ml). After stirring for 30 min, the above solution was transferred into a Teflon-lined autoclave (100 mL) and treated at 180 ˚C for 10 h. The product was recovered and rinsed with distilled water, then ethanol. After being dried at 60 ˚C for about 24h, the as-prepared sample was calcined in an oven at 500 ˚C for 2h.

NiO nanoparticle:$NiCl_2$•$6H_2O$ (107.3 mg) and hexamethylenetetramine (61.3 mg) were dissoloved in sodium citrate solution (0.7 Mm, 70 ml). After stirring for two days with slightly heated, the product was recovered and rinsed with distilled water, then ethanol. After being dried at 60 ˚C for about 24h, the as-prepared sample was calcined in an oven at 500 ˚C for 2h.

2.2. Structural analysis

The characterization of the as-prepared samples was carried out by X-ray diffraction (XRD, D/max 2500 PC) and transmission electron microscopy (TEM, FEI TecnaiG20). UV-vis diffused reflectance spectra were recorded on a UV 2450 spectrophotometer.

2.3. Photoelectrical performance

The photocathode semiconductor film was made by two-step doctor blade method on fluorine-doped tin oxide (FTO) conductive glass. NiO nanoparticles were coated directively on FTO as the first compact layer, following with NiO nano-flower, NiO slice-cluster and NiO nanoparticle, separately as the second light scattering layer. After calcination in air for 30 minutes at 500 ˚C, the NiO films were spin-coated with the perovskite solutions at 4000 rpm for 40 s, followed by heating at 100 °C for 5 min. The as prepared photocathodes were sandwiched together with the platinized counter electrodes and sealed with Surlyn film. The electrolyte was composed of 0.5 M LiI, 0.05 M I_2 and 0.5 M 4-tertbutylpyridine in acetonitrile. The active electrode area employed was approximately 0.25 cm^2. Zahner CIMPS-2 electrochemical workstation together with a Trusttech CHF-XM-500W source under simulated Sun illumination (Global AM 1.5, 100 mW cm^2) was used to test photocurrent-voltage (I-V) curves and electrochemical impedance spectra (EIS) (100 kHz to 0.1 Hz, 10 mV perturbation). Intensity-modulated photovoltage spectroscopy (IMVS) and intensity-modulated photocurrent spectroscopy (IMPS) were carried out using a Zahner CIMPS-2 system. The lamp-house was fitted with a blue light emitting diode (LED) (470 nm) driven by a PP210 (Zahner) frequency response analyser with a frequency range from 1000 Hz to 0.01 Hz.

3. RESULTS AND DISCUSSION

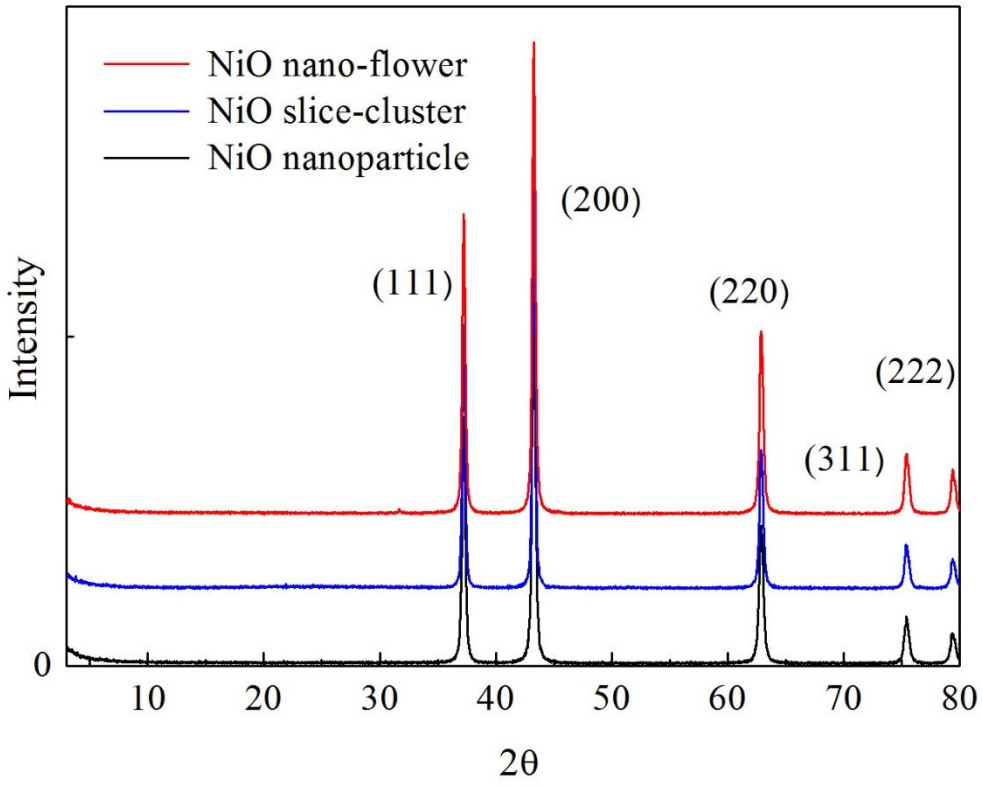

Figure 1. XRD patterns of NiO nano-flower, NiO slice-cluster and NiO nanoparticle.

Fig.1 shows the X-ray diffraction (XRD) data of NiO nano-flower, NiO slice-cluster and NiO nanoparticle. The appeared five sharp peaks of the three samples match well with cubic rock salt NiO phase (JCPDS file 778-429), which reveals the phase purity of the three samples. Also the strong peak intensities indicate the high crystallinity of the samples.

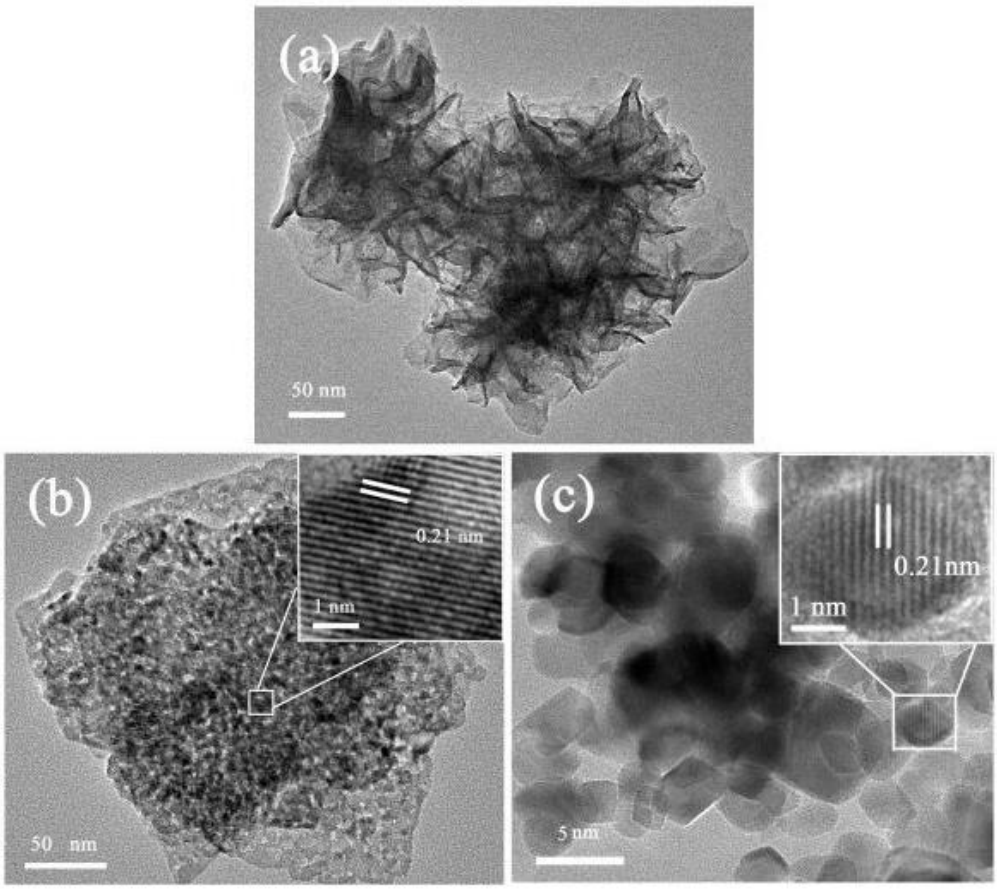

Figure 2. Typical TEM images of NiO nano-flower (a), NiO slice-cluster (b) and NiO nanoparticle (c).

TEM images of the as-prepared NiO nano-flower, NiO slice-cluster and NiO nanoparticle are shown in Fig 2. It can be clearly observed from Fig. 2a that the NiO nano-flowers are made up by several thin NiO nano-sheets crumpling into cluster. The diameter of the flower is about 200-300 nm. After treated by hydrothermal method, the morphology of the sample is changed as shown in Fig. 2b. NiO nano-particles are grouped together to form a slice, then piled up into NiO slice-cluster. The average diameter of the NiO nano-particle is about 5 nm and diameter of the NiO slice-cluster is about 200 nm. The crystal lattice fringes are clearly detected from high resolution TEM (HRTEM) and the lattice spacing is 0.21 nm, which can be indexed to the interplanar spacing of (200) crystal planes in cubic NiO [15]. This is consistent with XRD result. NiO nanoparticles are also prepared. From Fig. 2c, it can be seen that the diameter is about 3-5 nm, and a lattice spacing of 0.21 nm is observed from HRTEM, which is also indexed to (200) crystal planes of cubic NiO [15].

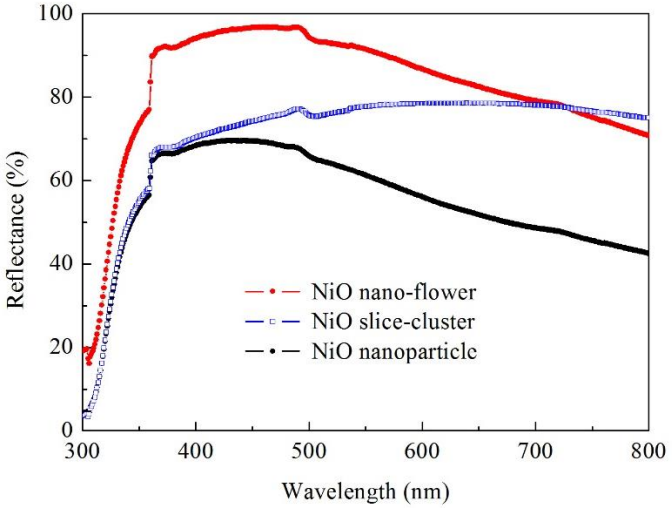

Figure 3. UV-vis diffused reflectance spectra of NiO nano-flower, NiO slice-cluster and NiO nanoparticle.

Fig. 3 shows the UV-vis diffused reflectance spectra of the samples. It is clearly that NiO nano-flowerpresents higher reflectance than NiO slice-cluster and NiO nanoparticle. NiO slice-cluster and NiO nanoparticle show almost the same reflectance from 300 to 400 nm. However, after 400 nm NiO slice-cluster shows much higher reflectance than NiO nanoparticle. Such result indicates that NiO nano-flowerowns a higher light scattering ability than the other two samples, which can be attributed to the unique morphology [19-20]. Therefore, more incident photons could be captured for useful transport and light harvesting efficiency could be improved. Such structure together with a high surface area can also improve the dye loading, which would increase the short current density and the photoelectric conversion efficiency.

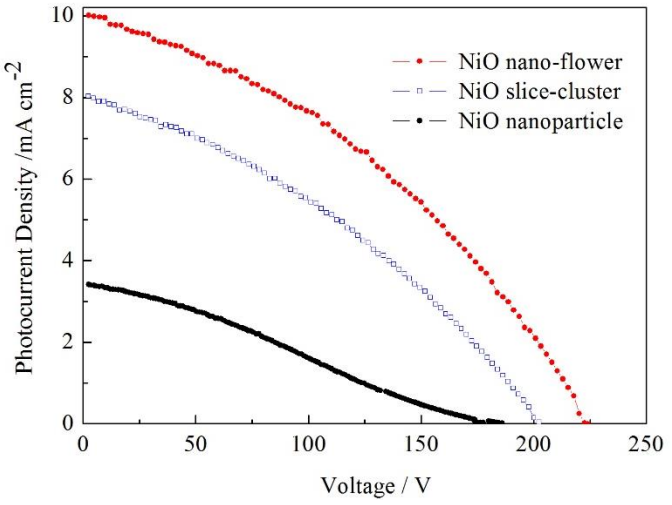

Figure 4. I-V curves for p-solar cellsbased on NiO nano-flower, NiO slice-cluster and NiO nanoparticle photocathodes. Illumination intensity of 100 mW cm^{-2} with AM 1.5 and an active area of 0.25 cm^2 were applied.

Fig. 4 shows the I-V curves of p-DSSCs with NiO nano-flower, NiO slice-cluster and NiO nanoparticle as photocathodes. Table 1 summarizes the measured and calculated values obtained. NiO nanoparticle shows relative low short circuit current density (J_{sc}) of 3.4 mA cm^{-2} and open circuit voltage (V_{oc}) of 186 mV. The calculated conversion efficiency (η) is only 0.17%. However, the parameters for the other two samples are highly improved especial for NiO nano-flower with J_{sc} of 10 mA cm^{-2}, V_{oc} of 224 mV and η of 0.84%. J_{sc} of NiO nano-flower is three times higher than that of NiO nanoparticle and η is 5 times enhanced. According to UV-vis results, NiO nano-flower shows a higher light scattering ability to absorb more light to increase the light harvest, which chould further increase the J_{sc} and η. Besides, NiO nano-flower presens a better fill factor (FF) (0.37) than that of NiO nanoparticle (0.27) which may be attributed to the reduced recombination of holes at the interface [20-21].

Table 1. Detailed photovoltaic parameters of p-DSSCs based on NiO nano-flower, NiO slice-cluster and NiO nanoparticle photocathodes.

Sample	J_{sc} (mA/cm^2)	V_{oc} (mV)	*FF*	*η*(%)
NiO nano-flower	10.0	224	0.37	0.84
NiO slice-cluster	8.0	202	0.35	0.57
NiO nanoparticle	3.4	186	0.27	0.17

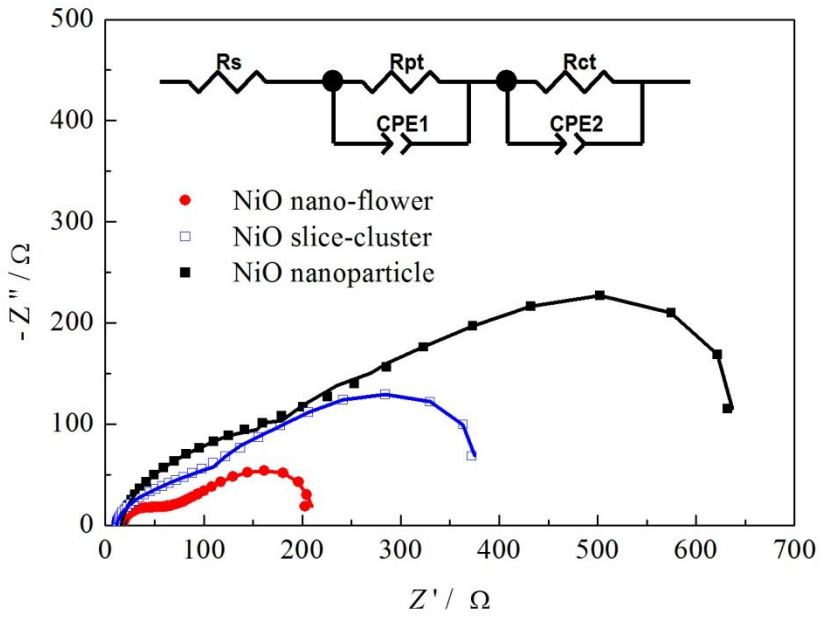

Figure 5. Nyquist plots of the p-DSSCs based on NiO nano-flower, NiO slice-cluster and NiO nanoparticle photocathodes. The inset shows the equivalent circuit for the impedance spectrum. Rs: serial resistance; Rpt: hole-transfer resistance of Pt electrode; Rct: hole-transfer resistance of photocathode; CPE: a constant phase element.

Electrochemical impedance spectra (EIS) ofthe three different p-DSSCs are shown in Fig. 5. Two semicircles on the EIS plots are observed, of which the one in the high frequency region is assigned to the resistance of the Pt/redox (I^-/I_3^-) interface hole transfer (R_{pt}) and the other one in the low frequency region is corresponded to the hole-transfer process occurring atthe NiO/dye/electrolyte interface (R_{ct}) [17,22-23]. Among the three samples, NiO nano-flower shows the lowest R_{pt} value and R_{ct} value, which indicates a superior hole transfer kinetics. The fitting results based on the equivalent circuit (Fig. 5, inset) [24-25] are summarized in Table 2. The order of total resistance is NiO nano-flower < NiO slice-cluster < NiO nanoparticle, which means NiO nano-flower can provide a better hole transport way and further an improved photoelectrochemical performance. This result is in agreement with the photoelectrochemical performance disscussed above.

Table 2. Fitted data from EIS spectra of p-DSSCs based on NiO nano-flower, NiO slice-cluster and NiO nanoparticle photocathodes.

	R_{pt} (Ω)	R_{ct} (Ω)	R (Ω)
NiO nano-flower	55	131	186
NiO slice-cluster	86	273	359
NiO nanoparticle	143	473	616

To further investigate the hole transport and recombination processes, intensity-modulated photocurrent spectroscopy (IMPS) and intensity-modulated photovoltage spectroscopy (IMVS) are used. The detailed IMPS/IMVS parameters are listed in Table 3 [20, 22, 26]. The hole transport time (τ_{tr}) for the three samples are almost the same, eventhough they present different morphologies, surface areas and traps/defects on the surface.It is reasonable to assume that the cover of solid $CH_3NH_3PbI_3$ layer on NiO surface wouldreduce lots of the surface traps/defects [14]. Thus the hole transport time could be reduced and be the same for the three samples. However, the hole life time (τ_h) of NiO nano-flower is much longer than that of NiO slice-cluster and NiO nanoparticle and the τ_{tr}/τ_h ratio of NiO nano-flower is much smaller than that of NiO slice-cluster and NiO nanoparticle, which means the less recombination in NiO nano-flower cells. The hole collection efficiency η_{cc} ($\eta_{cc} = 1-\tau_{tr}/\tau_h$) of the three samples are diffferent [27-28]. It is obvious that NiO nano-flower exhibits higher hole collection efficiency compared with the other two samples. And this can be contributed to the less recombination of NiO nano-flower.

Table 3. Detailed IMPS/IMVS parameters of p-DSSCs based on NiO nano-flower, NiO slice-cluster and NiO nanoparticle photocathodes.

	τ_{tr} (ms)	τ_h (ms)	η_{cc}
NiO nano-flower	16	64	0.75
NiO slice-cluster	18	40	0.55
NiO nanoparticle	18	28	0.36

4. CONCLUSIONS

In conclusion, NiO nano-flower, NiO slice-cluster and NiO nanoparticle are synthesized, of which NiO nano-flower used as photocathode of p-DSSC presents superior photoelectrochemical properties. A higher J_{sc} of 10 mA cm^{-2} and efficiency of 0.84% have been achieved by the NiO nano-flower p-DSSC. UV-vis diffused reflectance spectra indicates that NiO nano-flower owns strong light scatting and diffuse reflection to enhace light harvesting. EIS, IMPS and IMVS tests indicate that NiO nano-flower shows long hole life time, less recombinationand improved charge collection efficiency, which may due to its unique morphology. Besides, the hole transport time of all the samples are shortened, which may contribute to the less surface traps/defects improved by solid $CH_3NH_3PbI_3$ layer covering on NiO surface.

ACKNOWLEDGMENTS
This work has been supported by the National Natural Science Foundation of China (21301022 and 51303017) and Jiangsu Natural Science Foundation (BK20151187).

References

1. F. Odobel, L. L. Pleux, Y. Pellegrin, E. Blart, *Acc. Chem. Res*, 43(2010) 1063-1071.
2. F. Odobel, Y. Pellegrin, E. A. Gibson, A. Hagfeldt, A. L. Smeigh, L. Hammarström, *Coord. Chem. Rev,* 256 (2012) 2414-2423.
3. L. Li, E. A. Gibson, P. Qin, G. Boschloo, M. Gorlov, A. Hagfeldt, L. Sun, *Adv. Mater,* 22 (2010) 1759-1762.
4. Z. Ji, G. Natu, Z. Huang, Y. Wu, *Energy Environ. Sci,* 4 (2011) 2818-2821.
5. X. L. Zhang, Z. Zhang, D. Chen, P. Bäuerle, U. Bache, Y. -B. Cheng, *Chem. Commun,* 8 (2012) 9885-9887.
6. A. Renaud, B. Chavillon, L. Cario, L. L. Pleux, N. Szuwarski, Y. Pellegrin, E. Blart, E. Gautron, F. Odobel, S. Jobic, *J. Phys. Chem. C*, 117(2013) 22478-22483.
7. H. Wang, X. Zeng, Z. Huang, W. Zhang, X. Qiao, B. Hu, X. Zou, M. Wang, Y. -B. Cheng, W. Chen, *ACS Appl. Mater. Interfaces*, 6 (2014) 12609-12617.
8. F. Odobel, Y. Pellegrin, *J. Phys. Chem. Lett*, 4(2013) 2551-2564.
9. S. Powar, T. Daeneke, M. T. Ma, D. Fu, N. W. Duffy, G. Goetz, M. Weidelener, A. Mishra, P. Baeuerle, L. Spiccia, *Angew. Chem., Int. Ed*, 52 (2013) 602-605.
10. A. Yella, H. -W. Lee, H. N. Tsao, C. Yi, A. K. Chandiran, M. K. Nazeeruddin, E. W. -G. Diau, C. -Y. Yeh, S. M. Zakeeruddin, M. Grätzel, *Science*, 334 (2011) 629-634.
11. A. Yella, H. W. Lee, H. N. Tsao, C. Yi, A. K. Chandiran, M. K. Nazeeruddin, *Science*, 334 (2011) 629-634.
12. D. Ursu, M. Miclau, R. Banica, N. Vaszilcsin, *Mater. Lett*, 143 (2015) 91-93.
13. L. Lepleux, B. Chavillon, Y. Pellegrin, E. Blart, L. Cario, S. Jobic, F. Odobel, *Inorg. Chem*, 48 (2009) 8245-8250.
14. S. H. Kang, K. Zhu, N. R. Nealeb, A. J. Frank, *Chem. Commun*, 47 (2011) 10419-10421.
15. X. L. Zhang, F. Huang, A. Nattestad, K. Wang, D. Fu, A. Mishra, P. Bäuerle, U. Bach, Y. -B. Cheng, *Chem. Commun*, 47 (2011) 4808-4810.
16. A. Nattestad, A. J. Mozer, M. K. R. Fischer, Y. -B. Cheng, A. Mishra, P. Bäuerle, U. Bach, *Nat. Mater*, 9 (2010) 31-35.
17. L. D'Amario, G. Boschloo, A. Hagfeldt, L. Hammarström, *J. Phys. Chem. C*, 118 (2014) 19556-

19564.
18. M. Awais, D. D. Dowling, M. Rahman, J. G. Vos, F. Decker, D. Dini, *J. Appl. Electrochem*, 43 (2013) 191-197.
19. C. Cheng, Y. Shi, C. Zhu, W. Li, L. Wang, K. K. Fung, N. Wang, *Phys. Chem. Chem. Phys*, 13 (2011) 10631-10634.
20. J. Qu, Y. Yang, Q. Wu, P. R. Coxon, Y. Liu, X. He, K. Xi, N. Yuan, J. Ding, *RSC Adv*, 4 (2014) 11430-11437.
21. C. Y. Jiang, X. W. Sun, G. Q. Lo, D. L. Kwong, J. X. Wang, *Appl. Phys. Lett*, 90 (2007) 263501-3.
22. Z. Huang, G. Natu, Z. Ji, M. He, M. Yu, Y. Wu, *J. Phys. Chem. C*, 116 (2012) 26239-26246.
23. Q. Liu, L. Wei, S. Yuan, X. Ren, Y. Zhao, Z. Wang, M. Zhang, L. Shi, D. Li, A. Li, *RSC Adv*, 5 (2015) 71778-71784.
24. K. M. Lee, V. Suryanarayanan, K. C. Ho, *Sol. Energy Mater. Sol. Cells*, 91 (2007) 1416-1420.
25. G. Natu, Z. Huang, Z. Ji, Y. Wu, *Langmuir*, 28 (2012) 950-956.
26. J. Qu, G. R. Li and X. P. Gao, *Energy Environ. Sci*, 3 (2010) 2003-2009.
27. G. Schlichthorl, N. G. Park, A. J. Frank, *J. Phys. Chem. B*, 103 (1999) 782-791.
28. S. D. Stranks, G. E. Eperon, G. Grancini, C. Menelaou, M. J. P. Alcocer, T. Leijtens, L. M. Herz, A. Petrozza, H. J. Snaith, *Science*, 342 (2013) 341-344.